Brief Communication | Experimental and Others

http://dx.doi.org/10.3348/kjr.2016.17.5.725
pISSN 1229-6929 · eISSN 2005-8330
Korean J Radiol 2016;17(5):725-733

Korean Journal of Radiology
KJR

Evaluation of the Differences of Myocardial Fibers between Acute and Chronic Myocardial Infarction: Application of Diffusion Tensor Magnetic Resonance Imaging in a Rhesus Monkey Model

Yuqing Wang, PhD[1, 2*], Wei Cai, MD[1, 3*], Lei Wang, BD[1], Rui Xia, MD, PhD[1, 4], Wei Chen, MD, PhD[1, 5], Jie Zheng, PhD[6], Fabao Gao, MD, PhD[1]

[1]Department of Radiology, West China Hospital, Sichuan University, Sichuan 610041, China; [2]CAS Key Laboratory for Biomedical Effects of Nanomaterials and Nanosafety, National Center for Nanoscience and Technology of China, Beijing 100190, China; [3]Department of Radiology, Beijing Jishuitan Hospital, 4th Clinical Medical College of Peking University, Beijing 100035, China; [4]Department of Radiology, The First Affiliated Hospital, Chongqing Medical University, Chongqing 400016, China; [5]Department of Radiology, The First Affiliated Hospital of Kunming Medical University, Yunnan 650032, China; [6]Mallinckrodt Institute of Radiology, School of Medicine, Washington University, St. Louis, MO 63110, USA

Objective: To understand microstructural changes after myocardial infarction (MI), we evaluated myocardial fibers of rhesus monkeys during acute or chronic MI, and identified the differences of myocardial fibers between acute and chronic MI.

Materials and Methods: Six fixed hearts of rhesus monkeys with left anterior descending coronary artery ligation for 1 hour or 84 days were scanned by diffusion tensor magnetic resonance imaging (MRI) to measure apparent diffusion coefficient (ADC), fractional anisotropy (FA) and helix angle (HA).

Results: Comparing with acute MI monkeys (FA: 0.59 ± 0.02; ADC: 5.0 ± 0.6 x 10^{-4} mm^2/s; HA: 94.5 ± 4.4°), chronic MI monkeys showed remarkably decreased FA value (0.26 ± 0.03), increased ADC value (7.8 ± 0.8 x $10^{-4}$$mm^2/s$), decreased HA transmural range (49.5 ± 4.6°) and serious defects on endocardium in infarcted regions. The HA in infarcted regions shifted to more components of negative left-handed helix in chronic MI monkeys (-38.3 ± 5.0°–11.2 ± 4.3°) than in acute MI monkeys (-41.4 ± 5.1°–53.1 ± 3.7°), but the HA in remote regions shifted to more components of positive right-handed helix in chronic MI monkeys (-43.8 ± 2.7°–66.5 ± 4.9°) than in acute MI monkeys (-59.5 ± 3.4°–64.9 ± 4.3°).

Conclusion: Diffusion tensor MRI method helps to quantify differences of mechanical microstructure and water diffusion of myocardial fibers between acute and chronic MI monkey's models.

Keywords: *Rhesus monkey; Myocardial fiber; Myocardial infarction; Helix angle; Diffusion tensor MR imaging; DTI*

Received December 12, 2015; accepted after revision April 29, 2016.
This study was supported by the National Natural Science Foundation of China (81130027, 81301196).
*These authors contributed equally to this work.
Corresponding author: Fabao Gao, MD, PhD, Department of Radiology, West China Hospital, Sichuan University, No. 37 Guoxue Alley, Chengdu, Sichuan 610041, China.
• Tel: (8628) 85164108 • Fax: (8628) 85422135
• E-mail: gaofabao_sub@163.com

INTRODUCTION

Previous studies have confirmed that the deterioration of cardiac mechanical function originates from micro-alterations of myocardial fibers after myocardial infarction (MI) (1, 2). Compared with the conventional histological method, diffusion tenor magnetic resonance imaging (DT-MRI) is a highly sensitive approach to evaluate myocardial fibers in a 3D manner (3-5). However, *in-vivo* DT-MRI for myocardial fibers is limited by the image distortion that is induced by the cardiac motion and the amount of time required to complete the operation (6, 7). Alternatively, *ex-vivo* DT-MRI for animal models provides some valuable

insights into the evaluation of myocardial fibers after MI (8-11).

The *ex-vivo* DT-MRI method was used to evaluate the myocardial fibers of fixed hearts in different mammals (10-13). Compared with normal rats, the infarcted regions in chronic MI rats had significantly increased apparent diffusion coefficients (ADC), reduced fractional anisotropy (FA) and noticeably altered arrangements of myocardial fibers (12, 13). The structural damage and mechanical remodeling events during chronic MI significantly aided the understanding of the mechanical basis for and the prediction of the risk of arrhythmia and cardiac function failure (14, 15). However, the characteristics of myocardial fibers during acute MI were essential for the early diagnosis of cardiac function deterioration (1). In this study, we hypothesized that the diffusion and mechanical differences in myocardial fibers between acute and chronic MI could be quantified and differentiated using the *ex vivo* DT-MRI method.

The objective of this study was to quantify the characteristics of the myocardial fibers during acute and chronic MI, and subsequently identify the differences in myocardial fibers between acute and chronic MI in rhesus monkeys using the DT-MRI method, in order to understand the corresponding changes in patients with acute MI (16).

MATERIALS AND METHODS

Experiments

All experiments were performed in accordance with the

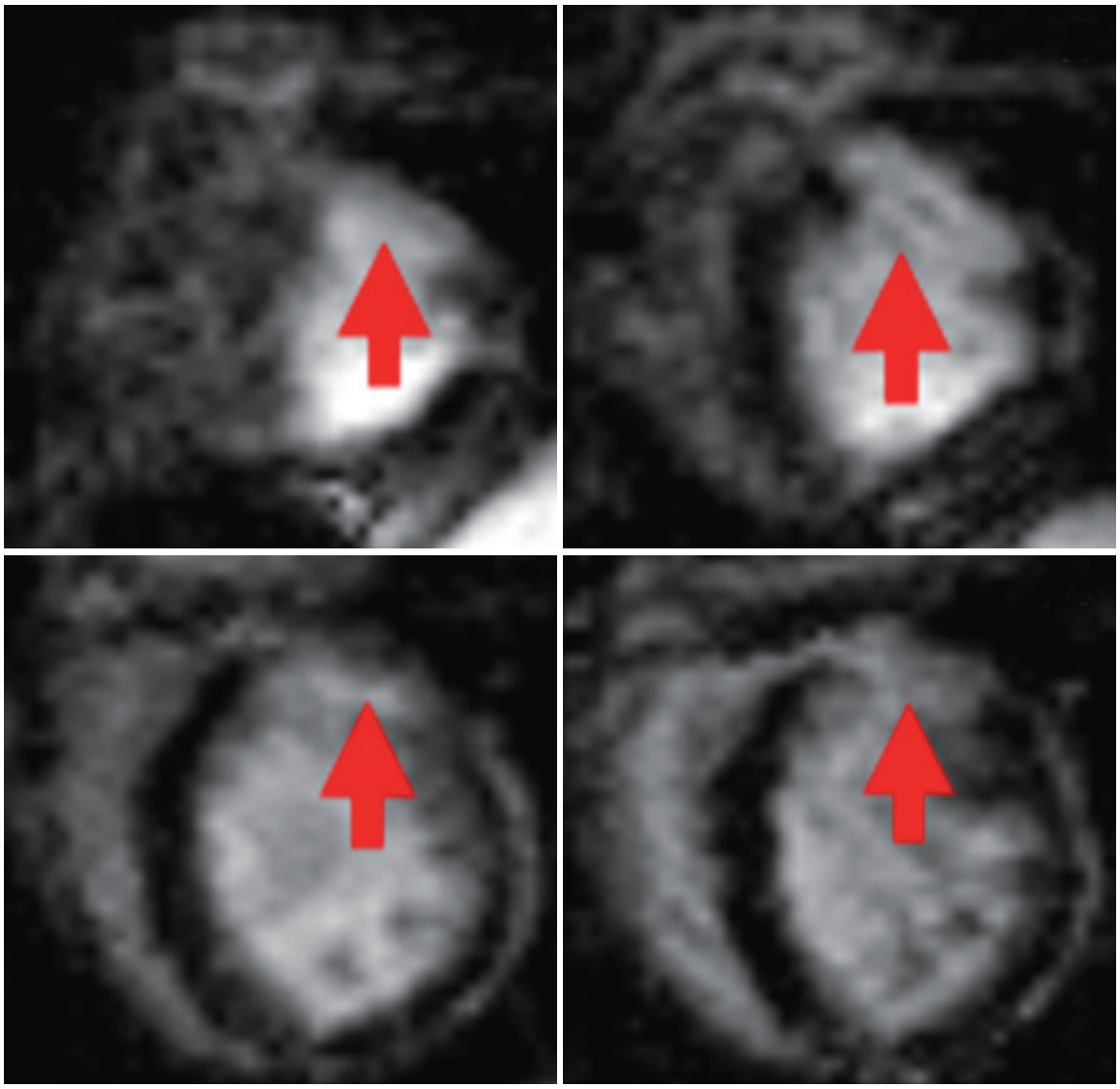

Fig. 1. Different slices of shot-axial DE-MRI. Hyperenhancement regions in anterior wall (red arrows) indicate infarcted regions. DE-MRI = delayed enhancement magnetic resonance imaging

Korean Journal of Radiology
KJR

guidelines set by the U.S. National Institute of Health and the regulations for the humane care of laboratory animals of our university. The study protocol was approved by the Institutional Review Committee on Animal Care of the provincial government.

Six adult rhesus monkeys (3 males and 3 females, aged 3 years) were randomized into the acute MI (n = 3) or the chronic MI (n = 3) group. All monkeys were anesthetized deeply by pentobarbital and underwent permanent suture ligation of the left anterior descending coronary artery. Monkey's chests were closed and fed for 1 hour or 84 days, named as MI-1 hour (n = 3) or MI-84 day (n = 3), respectively. Delayed enhancement magnetic resonance imaging (DE-MRI) was used to confirm infarcted regions in the left ventricular *in vivo* (Fig. 1). After two hours of completing DE-MRI, all infarcted monkeys were sacrificed and their hearts were excised under deep surgical anesthesia. All excised hearts were perfusion-fixed by a 4% paraformaldehyde solution and stored in a 1% paraformaldehyde solution.

Before DT-MRI scanning, Fomblin, special lubricating oil (per-fluororated poly ethers), was injected into four chambers of each excised heart to reduce susceptibility artifacts in myocardial margins during DT-MRI scanning, and then, each excised heart was sealed in a plastic container filled with Fomblin.

With the heart container in a 7T MR (Bruker BioSpec 70/30, Chengdu, China) scanner, DT-MRI was performed to evaluate the myocardial fibers after MI. The echo-planar imaging-based diffusion tensor sequence was applied to acquire a single non-weighted (B0) image and diffusion images in 30 gradient directions. The scanned parameters were listed as follows: repetition time/echo time = 12000/32 ms, matrix = 100 x 100, field of view = 50 x 50 mm, slice thickness = 0.8 mm, flip angle = 90°, segment = 16, number of excitation = 25 and b value = 1300 ms/μm^2. After DT-MRI, the hearts were sectioned and fixed, and infarcted regions and orientations of myocardial fibers were observed by Masson staining.

Data Analysis

Before calculating the parameters of DT-MRI, the diffusion images in 30 gradient directions were re-aligned with the B0 image to correct the movement errors due to mild scanner vibration (17-19). This step was taken with in-house programs that were encoded using the MATLAB platform (MathWorks, Natick, MA, USA). Afterwards, the singular value decomposition method was employed to calculate three eigenvectors and the corresponding eigenvalues of each voxel in the myocardial tissues, which were essential for the subsequent analysis of the various characteristics of the myocardial fibers.

The FA values and ADC values were calculated by voxel-based three eigenvalues to quantify the diffusion characteristics of the myocardial fibers. This step was performed using the diffusion toolkit package (Massachusetts General Hospital, Boston, MA, USA).

The voxel-based tensors and the helix angle (HA) were

Table 1. All Parameters in Infarcted Regions and Remote Regions

Group	Number	FA	ADC	Range of HA
MI-1 hour (infarcted)	Mean	0.59 ± 0.02	5.0 ± 0.6 x 10^{-4} mm^2/s	94.5 ± 4.4° (-41.4 ± 5.1°–53.1 ± 3.7°)
	1	0.61	4.6 x 10^{-4} mm^2/s	98.6° (-42.2°–56.4°)
	2	0.59	5.3 x 10^{-4} mm^2/s	95.2° (-46.0°–49.2°)
	3	0.58	5.8 x 10^{-4} mm^2/s	89.8° (-36.0°–53.8°)
MI-1 hour (remote)	Mean	0.62 ± 0.03	4.8 ± 0.8 x 10^{-4} mm^2/s	124.4 ± 3.2° (-59.5 ± 3.4°–64.9 ± 4.3°)
	1	0.65	3.8 x 10^{-4} mm^2/s	127.7° (-61.6°–66.1°)
	2	0.59	5.3 x 10^{-4} mm^2/s	121.4° (-61.3°–60.1°)
	3	0.60	5.2 x 10^{-4} mm^2/s	124.0° (-55.5°–68.5°)
MI-84 days (infarcted)	Mean	0.26 ± 0.03	7.8 ± 0.8 x 10^{-4} mm^2/s	49.5 ± 4.6° (-38.3 ± 5.0°–11.2 ± 4.3°)
	1	0.25	8.2 x 10^{-4} mm^2/s	49.0° (-42.5°–6.5°)
	2	0.3	6.9 x 10^{-4} mm^2/s	54.4° (-39.6°–14.8°)
	3	0.24	8.4 x 10^{-4} mm^2/s	45.2° (-32.8°–12.4°)
MI-84 days (remote)	Mean	0.59 ± 0.02	4.9 ± 0.7 x 10^{-4} mm^2/s	110.3 ± 3.6° (-43.8 ± 2.7°–66.5 ± 4.9°)
	1	0.58	5.4 x 10^{-4} mm^2/s	106.3° (-43.2°–63.1°)
	2	0.62	4.1 x 10^{-4} mm^2/s	113.5° (-41.4°–72.1°)
	3	0.58	5.3 x 10^{-4} mm^2/s	111.1° (-46.7°–64.4°)

ADC = apparent diffusion coefficients, FA = fractional anisotropy, HA = helix angle, MI = myocardial infarction

calculated by voxel-based primary eigenvectors to quantify the mechanical and microstructural characteristics of the myocardial fibers. This step was taken with in-house programs that were encoded using the MATLAB platform (MathWorks, Natick, MA, USA).

RESULTS

The FA, HA, and ADC values of each monkey and the mean values were listed in Table 1. Figure 2 illustrated FA and ADC maps of the infarcted slices in the MI-1 hour and MI-84 day monkeys. In the group of MI-1 hour monkeys, compared with the remote regions (FA: 0.62 ± 0.03, ADC: 4.8 ± 0.8 x 10^{-4} mm^2/s), the MI regions (red arrow) showed slightly decreased FA (0.59 ± 0.02) and increased ADC values (5.0 ± 0.6 x 10^{-4} mm^2/s), which are involved in early intracellular edema of the myocytes. In contrast, in the group of MI-84 days monkeys, compared with the remote regions (FA: 0.59 ± 0.02, ADC: 4.9 ± 0.7 × 10^{-4} mm^2/s), the MI regions (red arrow) showed noticeably decreased FA (0.26 ± 0.03) and increased ADC values (7.8 ± 0.8 x 10^{-4} mm^2/s), which indicated severity of necrotic myocytes.

Figure 3 is the HA and tensor map of the infarcted slices in the MI-1 hour and MI-84 days monkeys. In the group of MI-1 hour monkeys, compared with the remote regions (HA: 124.4 ± 3.2°), there were mild changes in the HA transmural ranges (94.5 ± 4.4°) of the infarcted region (black circle) and the primary orientations of the tensor. The tensors became slightly thinner in the endocardium but not in the epicardium. In contrast, the HA values (remote regions: 110.3 ± 3.6°, infarcted regions: 49.5 ± 4.6°) in the MI-84 days monkeys were not homogeneous. Extensive tissue defects were observed in the endocardium. The decreased HA indicated the reduced mechanical function

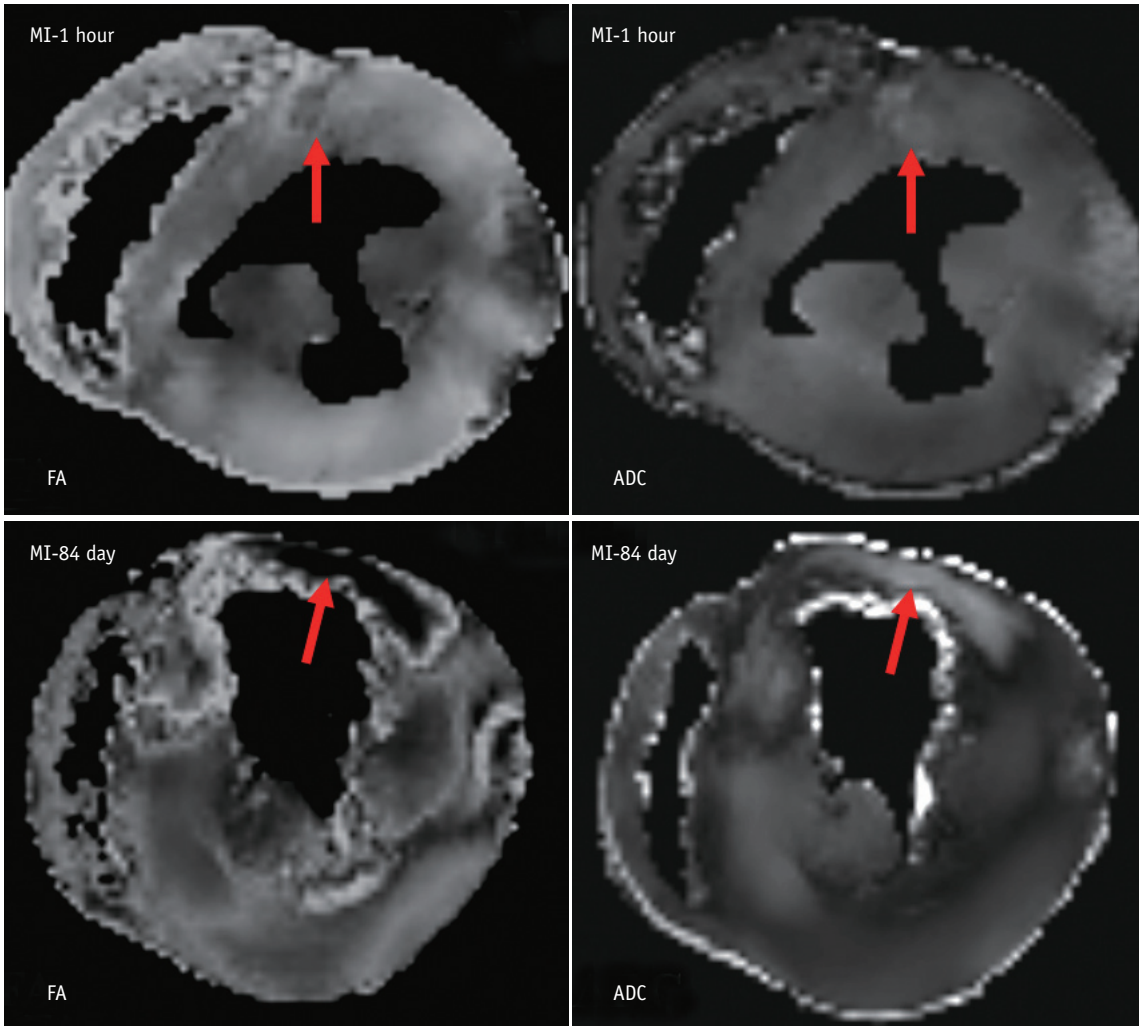

Fig. 2. Diffusion maps of myocardial fibers. Regions pointed by red arrows are MI regions. ADC = apparent diffusion coefficients, FA = fractional anisotropy, MI = myocardial infarction

Korean Journal of Radiology
KJR

and the increased electrophysiological risk in the infarcted regions.

Figure 4 enables the comparison of the tensor map with the Masson staining image. The MI-1 hour panel showed that the density of the myocardial fibers decreased slightly. The tensor map also showed a slightly decreased arrangement and density of the tensors in the myocardial fibers. The Masson staining image in the MI-84 days panel showed an expansive area of blue collagens and myocardial fibers in the blue collagens that are sparsely distributed. The tensor map showed some defects of the tensors in the endocardium.

Figure 5 illustrated the transmural range of HA from the epicardium to the endocardium on the anterior and posterior walls in the MI-1 hour and MI-84 days monkeys. Compared with the MI-1 hour monkeys (infarcted: -41.4 ± 5.1°–53.1 ± 3.7°, remote: -59.5 ± 3.4°–64.9 ± 4.3°), the infarcted regions in the MI-84 days monkeys showed a significantly decreased HA transmural range and a significant shift of the HA transmural range from the double-helix to the left-handed helix (-38.3 ± 5.0°–11.2 ± 4.3°), but the remote regions showed a significant shift of the HA transmural range from the double-helix to the right-handed helix (-43.8 ± 2.7°–66.5 ± 4.9°). The changed HA transmural range indicated decreased wall torsion in the infarcted regions and mechanical compensation in the remote region.

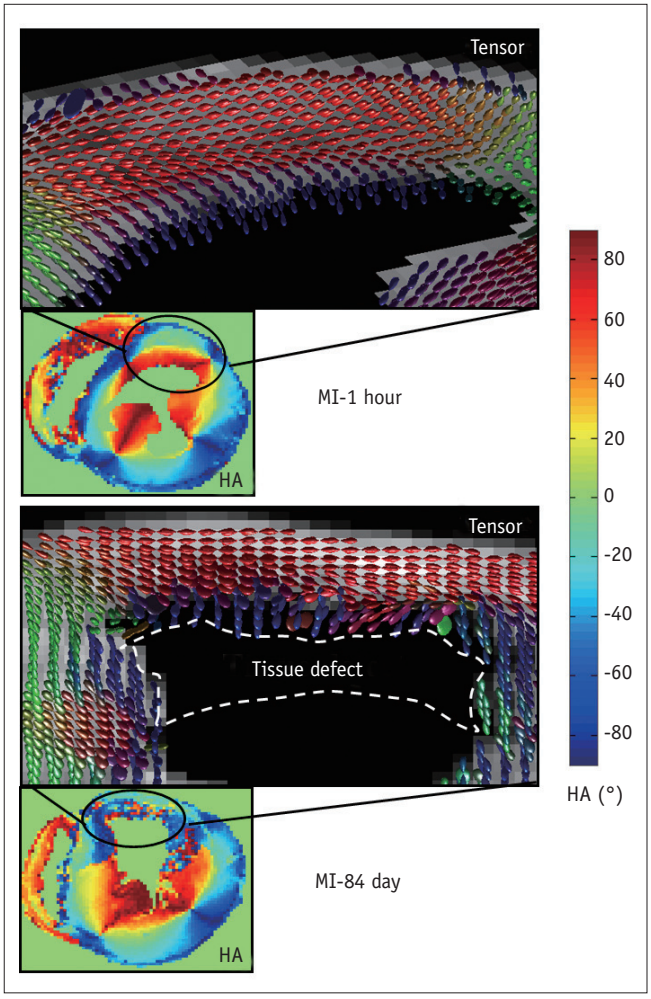

Fig. 3. HA and tensor maps. MI-1 hour monkeys show slight changes in HA values and primary orientations of tensors in infarcted regions (marked by black circles). MI-84 days monkeys show severely inhomogeneous HA values, very few positive right-handed HA values and irregular primary orientations of tensors in infarcted regions. Large area of defects can be seen in endocardium. HA = helix angle, MI = myocardial infarction

DISCUSSION

In this study, the DT-MRI method was applied successfully to quantify the characteristics of myocardial fibers in rhesus monkeys with acute and chronic MI. Our results confirmed that there were differences in myocardial tensor and diffusion between the acute and chronic MI monkey models. Moreover, our findings provided a more comprehensive understanding of the early changes of myocardial fibers in patients with acute MI.

Diffusion Parameters: FA and ADC Values

The FA value is considered as the longitudinal-to-transverse aspect ratio of the myocytes (6, 20). During the MI-1 hour period, many spherical cells such as inflammatory cells, swollen myocytes and myofibroblasts began to accumulate in the infarcted regions, which slightly reduced the FA values in the infarcted regions due to the slight reduction of the longitudinal-to-transverse ratio of the myocytes. When the time was extended to MI-84 days, the myocardial fibers in the scar tissues became disarrayed, and extensive collagens replaced the extracellular matrix in the infarcted regions, which resulted in the severe reduction of the FA values in the infarcted regions. Our findings were consistent with those from a previous histological study; more severe MI revealed lower FA values in the infarcted regions (12, 21).

The ADC value was used to quantify the balance of free water between the intracellular and extracellular space volumes (6). During the MI-1 hour, the increased lactic acid damaged the protein in the infarcted region, and the combined water in the protein became free water; subsequently, the elevated osmotic pressures caused by the intracellular Na+ accumulation caused the free water

to enter into the intracellular space due to dysfunctions of the Na+/K+ channels (22, 23). Compared with the remote regions, the infarcted region showed a slight increment of free water in the intracellular space, which mildly increased the ADC values in the infarcted regions. In the MI-84 days, the extracellular space in the infarcted regions was increased significantly since the aggregations of fibroblasts, neutrophils, and macrophages did not fill the extracellular space created by the necrotic myocytes after MI (6). Accordingly, the significantly increased ADC values were attributed to the increased extracellular space in the infarcted regions.

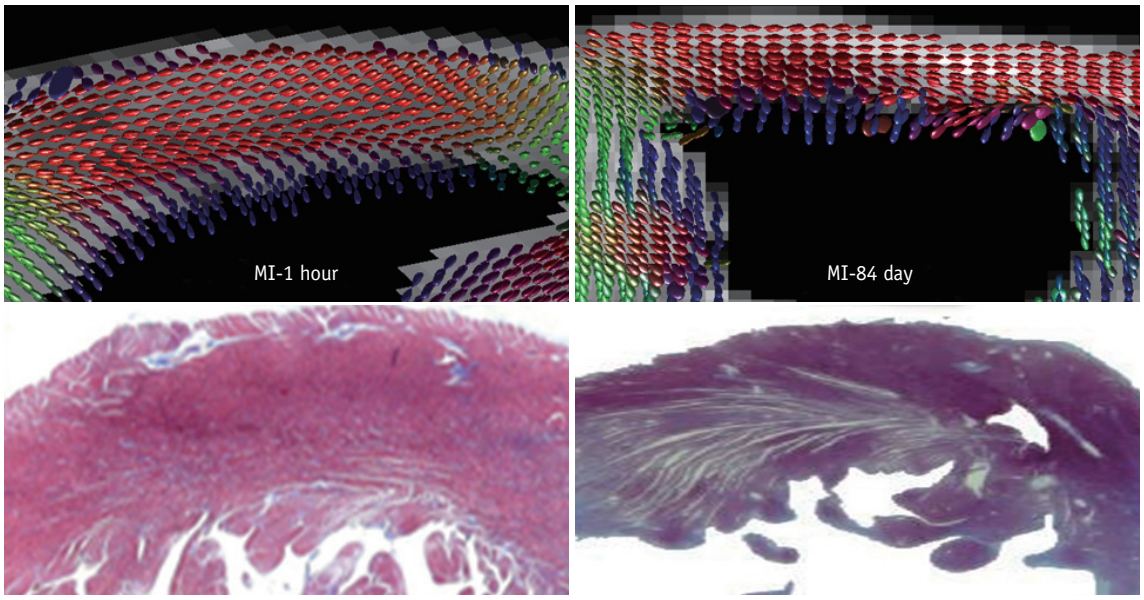

Fig. 4. Comparison between tensor maps and Masson's staining images. On MI-1 hour panel, orientations of myocardial fibers remain consistent. Tensor map also reveals similar arrangements and density of tensors in myocardial fibers. On MI-84 days panel, Masson's staining image shows large area of blue collagens, myocardial fibers in blue collagens are sparsely distributed, and orientation of myocardial fibers are inhomogeneous. Tensor map displays some tissue defects of tensors in endocardium and tensors are irregularly arranged. MI = myocardial infarction

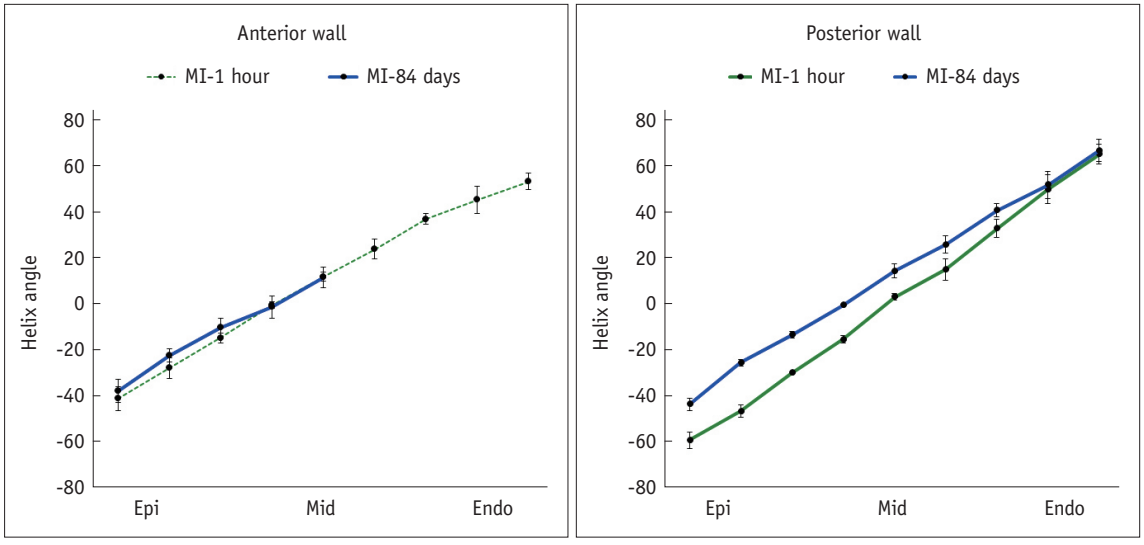

Fig. 5. Remodeling process of HA transmural range from epicardium to endocardium on anterior and posterior walls during MI-1 hour and MI-84 days monkeys. HA transmural range in infarcted region (anterior) is decreased but shift from double-helix toward left-handed helix during chronic MI. However, HA transmural range in remote (posterior) region shows increased shift from double-helix toward right-handed helix during chronic MI. HA = helix angle, MI = myocardial infarction

Korean Journal of Radiology
KJR

Mechanical Parameters: Tensors and HA Values

The voxel-based tensors are the important mechanical microstructures in the myocardial fibers because the wall torsion depends on the movements of the multi-orientation tensors (16, 24). In the MI-1 hour, the early stage of myocardial ischemia resulted in moderate myocardial edema, but the capillary wall retained its structural integrity, and the myocytes did not undergo extensive apoptosis. In the MI-84 days, injury on the infarcted wall was transmural from the endocardium to the epicardium. Some tissue defects of the myocardial tensors occurred in the endocardium of the infarcted wall. The scar and collagens in the residual wall resulted in the irregular arrangements of the tensors, which significantly increased the electrophysiological risk (14).

The transmural range of HA was widely applied to quantify the orientations of myocardial fibers from the epicardium to the endocardium (25-31). In the MI-1 hour, the change in the transmural range of HA was moderate as the orientations of the tensors remained essentially unchanged in the infarcted region. In the MI-84 days, the transmural range of HA was significantly reduced due to tissue defects of the tensors on the endocardium. The tissue defects on the endocardium resulted in the reduction of the positive right-handed helix in the infarcted regions, which revealed the shift from the transmural double-helix to the residual negative left-handed helix on the epicardium. However, the remote regions revealed the shift from the transmural double-helix to the reduced negative left-handed helix on the epicardium. Our findings in rhesus monkeys were consistent with the findings of previous studies that were conducted using other animals (6, 12, 32-34). We proposed that the HA shifts during MI-84 day were indicative of decreased wall torsion and contractile efficiency in the infarcted and mechanical compensation in the remote region (35).

Moreover, the FA values, ADC values or transmural range of HA in the infarcted regions were approximately 0.26, 0.00078 mm^2/s or -38 ± 11° in the MI-84 days monkeys, respectively, and the values were close to those in the MI patients (0.26, 0.000824 mm^2/s or -36 ± 10°) (6, 12, 21, 32-34). Thus, the mild changes of water diffusion and myocardial tensors in the MI-1 hour monkeys could contribute to the understanding and evaluation of these parameters in patients during the early stage of acute MI.

Limitations

More monkeys should be recruited in our future study. Formalin fixation decreased *ex-vivo* diffusion of myocardium (36-38). The effect of temperature on *ex-vivo* diffusion of myocardium might be increased due to the increased coil temperature caused by the long scanning period.

In conclusion, our study confirmed that the DT-MRI method could quantify and identify the acute and chronic MI monkey models by comparing the mechanical microstructure and water diffusion of myocardial fibers. According to the similar changes between monkeys and chronic MI patients, the characteristics of myocardial fibers in the acute MI monkeys could contribute to the understanding and evaluation of these parameters in patients during the early stage of acute MI.

REFERENCES

1. Vadakkumpadan F, Arevalo H, Trayanova NA. Patient-specific modeling of the heart: estimation of ventricular fiber orientations. *J Vis Exp* 2013 Jan 8 [Epub]. http://dx.doi.org/10.3791/50125
2. Lakshmanan R, Krishnan UM, Sethuraman S. Living cardiac patch: the elixir for cardiac regeneration. *Expert Opin Biol Ther* 2012;12:1623-1640
3. Wang Y, Haynor DR, Kim Y. An investigation of the importance of myocardial anisotropy in finite-element modeling of the heart: methodology and application to the estimation of defibrillation efficacy. *IEEE Trans Biomed Eng* 2001;48:1377-1389
4. Niederer SA, Buist ML, Pullan AJ, Smith NP. Computing work in the ischemic heart. *Conf Proc IEEE Eng Med Biol Soc* 2004;5:3646-3649
5. Vetter FJ, McCulloch AD. Three-dimensional analysis of regional cardiac function: a model of rabbit ventricular anatomy. *Prog Biophys Mol Biol* 1998;69:157-183
6. Wu MT, Tseng WY, Su MY, Liu CP, Chiou KR, Wedeen VJ, et al. Diffusion tensor magnetic resonance imaging mapping the fiber architecture remodeling in human myocardium after infarction: correlation with viability and wall motion. *Circulation* 2006;114:1036-1045
7. Wu MT, Su MY, Huang YL, Chiou KR, Yang P, Pan HB, et al. Sequential changes of myocardial microstructure in patients postmyocardial infarction by diffusion-tensor cardiac MR: correlation with left ventricular structure and function. *Circ Cardiovasc Imaging* 2009;2:32-40, 6 p following 40
8. Peyrat JM, Sermesant M, Pennec X, Delingette H, Xu C, McVeigh ER, et al. *Statistical comparison of cardiac fibre architectures*. In: Sachse FB, Seemann G, eds. *Functional imaging and modeling of the heart: 4th International Conference, Salt Lake City, UT, USA, June 7-9, 2007. Lecture notes in computer science, Vol 4466*. Berlin, Heidelberg: Springer Berlin Heidelberg, 2007:413-423
9. Jiang Y, Guccione JM, Ratcliffe MB, Hsu EW. Transmural

heterogeneity of diffusion anisotropy in the sheep myocardium characterized by MR diffusion tensor imaging. *Am J Physiol Heart Circ Physiol* 2007;293:H2377-H2384
10. Healy LJ, Jiang Y, Hsu EW. Quantitative comparison of myocardial fiber structure between mice, rabbit, and sheep using diffusion tensor cardiovascular magnetic resonance. *J Cardiovasc Magn Reson* 2011;13:74
11. Mekkaoui C, Huang S, Chen HH, Dai G, Reese TG, Kostis WJ, et al. Fiber architecture in remodeled myocardium revealed with a quantitative diffusion CMR tractography framework and histological validation. *J Cardiovasc Magn Reson* 2012;14:70
12. Chen J, Song SK, Liu W, McLean M, Allen JS, Tan J, et al. Remodeling of cardiac fiber structure after infarction in rats quantified with diffusion tensor MRI. *Am J Physiol Heart Circ Physiol* 2003;285:H946-H954
13. Sosnovik DE, Wang R, Dai G, Wang T, Aikawa E, Novikov M, et al. Diffusion spectrum MRI tractography reveals the presence of a complex network of residual myofibers in infarcted myocardium. *Circ Cardiovasc Imaging* 2009;2:206-212
14. Hooks DA, Trew ML, Caldwell BJ, Sands GB, LeGrice IJ, Smaill BH. Laminar arrangement of ventricular myocytes influences electrical behavior of the heart. *Circ Res* 2007;101:e103-e112
15. Desai KV, Laine GA, Stewart RH, Cox CS Jr, Quick CM, Allen SJ, et al. Mechanics of the left ventricular myocardial interstitium: effects of acute and chronic myocardial edema. *Am J Physiol Heart Circ Physiol* 2008;294:H2428-H2434
16. Yang P, Han P, Hou J, Zhang L, Song H, Xie Y, et al. Electrocardiographic characterization of rhesus monkey model of ischemic myocardial infarction induced by left anterior descending artery ligation. *Cardiovasc Toxicol* 2011;11:365-372
17. Mohammadi S, Freund P, Feiweier T, Curt A, Weiskopf N. The impact of post-processing on spinal cord diffusion tensor imaging. *Neuroimage* 2013;70:377-385
18. Savadjiev P, Strijkers GJ, Bakermans AJ, Piuze E, Zucker SW, Siddiqi K. Heart wall myofibers are arranged in minimal surfaces to optimize organ function. *Proc Natl Acad Sci U S A* 2012;109:9248-9253
19. Geerts L, Bovendeerd P, Nicolay K, Arts T. Characterization of the normal cardiac myofiber field in goat measured with MR-diffusion tensor imaging. *Am J Physiol Heart Circ Physiol* 2002;283:H139-H145
20. Holmes AA, Scollan DF, Winslow RL. Direct histological validation of diffusion tensor MRI in formaldehyde-fixed myocardium. *Magn Reson Med* 2000;44:157-161
21. Wu Y, Zhang LJ, Zou C, Tse HF, Wu EX. Transmural heterogeneity of left ventricular myocardium remodeling in postinfarct porcine model revealed by MR diffusion tensor imaging. *J Magn Reson Imaging* 2011;34:43-49
22. Kuntz ID Jr, Brassfield TS, Law GD, Purcell GV. Hydration of macromolecules. *Science* 1969;163:1329-1331
23. Kloner RA, Rude RE, Carlson N, Maroko PR, DeBoer LW, Braunwald E. Ultrastructural evidence of microvascular damage and myocardial cell injury after coronary artery occlusion: which comes first? *Circulation* 1980;62:945-952
24. Barmpoutis A, Vemuri BC. A unified framework for estimating diffusion tensors of any order with symmetric positive-definite constraints. *Proc IEEE Int Symp Biomed Imaging* 2010:1385-1388
25. Helm PA, Younes L, Beg MF, Ennis DB, Leclercq C, Faris OP, et al. Evidence of structural remodeling in the dyssynchronous failing heart. *Circ Res* 2006;98:125-132
26. Tseng WY, Dou J, Reese TG, Wedeen VJ. Imaging myocardial fiber disarray and intramural strain hypokinesis in hypertrophic cardiomyopathy with MRI. *J Magn Reson Imaging* 2006;23:1-8
27. Ripplinger CM, Li W, Hadley J, Chen J, Rothenberg F, Lombardi R, et al. Enhanced transmural fiber rotation and connexin 43 heterogeneity are associated with an increased upper limit of vulnerability in a transgenic rabbit model of human hypertrophic cardiomyopathy. *Circ Res* 2007;101:1049-1057
28. Helm PA, Tseng HJ, Younes L, McVeigh ER, Winslow RL. Ex vivo 3D diffusion tensor imaging and quantification of cardiac laminar structure. *Magn Reson Med* 2005;54:850-859
29. Lombaert H, Peyrat JM, Croisille P, Rapacchi S, Fanton L, Cheriet F, et al. Human atlas of the cardiac fiber architecture: study on a healthy population. *IEEE Trans Med Imaging* 2012;31:1436-1447
30. Toussaint N, Sermesant M, Stoeck CT, Kozerke S, Batchelor PG. In vivo human 3D cardiac fibre architecture: reconstruction using curvilinear interpolation of diffusion tensor images. *Med Image Comput Comput Assist Interv* 2010;13(Pt 1):418-425
31. Rohmer D, Sitek A, Gullberg GT. Reconstruction and visualization of fiber and laminar structure in the normal human heart from ex vivo diffusion tensor magnetic resonance imaging (DTMRI) data. *Invest Radiol* 2007;42:777-789
32. Benson AP, Bernus O, Dierckx H, Gilbert SH, Greenwood JP, Holden AV, et al. Construction and validation of anisotropic and orthotropic ventricular geometries for quantitative predictive cardiac electrophysiology. *Interface Focus* 2011;1:101-116
33. Vadakkumpadan F, Arevalo H, Prassl AJ, Chen J, Kickinger F, Kohl P, et al. Image-based models of cardiac structure in health and disease. *Wiley Interdiscip Rev Syst Biol Med* 2010;2:489-506
34. Wu EX, Wu Y, Nicholls JM, Wang J, Liao S, Zhu S, et al. MR diffusion tensor imaging study of postinfarct myocardium structural remodeling in a porcine model. *Magn Reson Med* 2007;58:687-695
35. Liu W, Ashford MW, Chen J, Watkins MP, Williams TA, Wickline SA, et al. MR tagging demonstrates quantitative differences in regional ventricular wall motion in mice, rats, and men. *Am J Physiol Heart Circ Physiol* 2006;291:H2515-H2521
36. Guilfoyle DN, Helpern JA, Lim KO. Diffusion tensor imaging in fixed brain tissue at 7.0 T. *NMR Biomed* 2003;16:77-81
37. Sun SW, Neil JJ, Liang HF, He YY, Schmidt RE, Hsu CY, et

al. Formalin fixation alters water diffusion coefficient magnitude but not anisotropy in infarcted brain. *Magn Reson Med* 2005;53:1447-1451

38. Aggarwal M, Zhang J, Pletnikova O, Crain B, Troncoso J, Mori S. Feasibility of creating a high-resolution 3D diffusion tensor imaging based atlas of the human brainstem: a case study at 11.7 T. *Neuroimage* 2013;74:117-127